JOURNAL OF SOLID STATE CHEMISTRY 70, 36–47 (1987)

Characterization of a Mixed-Chains One-Dimensional Compound*

A. MEERSCHAUT,† P. GRENOUILLEAU, L. GUÉMAS, AND J. ROUXEL

Laboratoire de Chimie des Solides, U.A. du CNRS n°279, Université de Nantes, 2, rue de la Houssinière, 44072 Nantes Cédex, France

Received December 1, 1986; in revised form February 11, 1987

The new ternary $Nb_3Se_{10}Br_2$ compound has been prepared and structurally characterized. It crystallizes in the orthorhombic system, *Ibca* space group, with unit cell parameters $a = 14.205(3)$ Å, $b = 23.722(4)$ Å, $c = 38.243(8)$ Å, $Z = 32$. The structure exhibits two types of infinite chains centered on the 2 or 2_1 axes; such an arrangement is reminiscent of what is observed in parent chain-like compounds as $(MSe_4)_nI$. This compound is a diamagnetic semiconductor with $E_a = 0.34$ eV. © 1987 Academic Press, Inc.

Introduction

There is an ever increasing number of diverse physical phenomena to be found in low-dimensional solids. Then, there is a need for new materials to experimentally support the growing development of theories (*1, 2*).

Unfortunately the synthesis of new low-dimensional solids can be difficult. In low-dimensional compounds, there is a van der Waals gap separating atomically identical (usually anionic) sheets or fibers in the two- and one-dimensional cases, respectively. As a result there is a tendency for chain–chain (or layer–layer) repulsion to fix, in the main, the true dimensionality of the system. For example, TaS_3 which is more ionic than $NbSe_3$ is also more one-dimensional in character (*2*): there, important pretransitional effects can be observed before a transition which goes as far as a metal to nonmetal transition.

Such an evolution which associates the strongest 1-D character to the most ionic chains places, of course, a limit on the stability of the overall structure. For a given structural type to be stable the bonding through the van der Waals gap, usually rather weak, must stabilize the structure against the repulsion between similar atomic layers situated on each side. In the case of oxides this repulsion is strong and destabilizing: most of the MO_2 phases have the rutile structure and not the layered structure of the parent MS_2 or MSe_2 chalcogenides. High oxidation states of transition metals having the ability to sufficiently polarize oxygen toward the inside of the slabs are necessary to allow a layered structure (MoO_3). On the other hand, tellurides are always highly covalent and often quasi-metallic compounds. The chalcogen-rich sulfides and selenides represent the best domain in chemistry to find 1-D and 2-D materials.

Until now, the majority of 1-D chalcogenides consisted of chains, either with in-

* Dedicated to Dr. Franz Jellinek.

† To whom all correspondence should be addressed.

0022-4596/87 $3.00

Copyright © 1987 by Academic Press, Inc.
All rights of reproduction in any form reserved.

terchain coupling which thus creates highly anisotropic sheets (as in $NbSe_3$) or with chains stabilized by counterions which separate and minimize chain–chain repulsions. The latter point is well illustrated by the fact that individual $[VS_4]$ chains exist in VS_4 (*3*) but that, due to an increased ionicity, NbS_4 and TaS_4 cannot be prepared. One has to separate the chains by iodine, like in $(MX_4)_nI$ phases (*4*). In this work we report a new structure type in which the geometrical role of the counterion has been assumed, for the first time, by another chain of different composition.

Experimental

A parallelepipedic-shaped crystal of fibrous aspect was selected from a crystalline bulk obtained by heating niobium powder (99.9%, Koch Light), selenium pellets (99.999%, Ventron), and bromine (Carlo Erba 99.5%) in a 1 : 3 : 1 ratio in an evacuated Pyrex tube for 2 weeks at 500°C.

A preliminary X-ray study with Laüe and Weissenberg photographs gave unambiguously an orthorhombic symmetry with the *Ibca* space group. The unit cell parameters a = 14.205(3) Å, b = 23.722(4) Å, and c = 38.243(8) Å were refined from Guinier powder data from the first 50 reflections (Guinier–Nonius camera FR552, quartz crystal monochromator, Cu$K\alpha_1$ = 1.54056 Å, Si as internal standard). The powder pattern, given in Table I, includes observed and calculated interplanar distances, along with the intensities calculated from the Lazy Pulverix program (*5*).

Similar unit cell parameters were obtained by Rijnsdorp (*6*) for one of the numerous phases that were recognized in the course of the study of the Nb–Se–Br system, but neither the composition nor the crystal structure was given.

The real composition is not $NbSe_3Br$ as could be inferred from the starting Nb/Se/Br ratios used in the preparation. A microprobe analysis on a crystal, performed at five different points, reveals uniform values which lead to the $Nb_3Se_{10}Br_2$ formulation (Table II). This result, in addition, was confirmed on two other crystals.

TABLE I

$Nb_3Se_{10}Br_2$—X-RAY POWDER DIFFRACTION DATA

hkl	$d_{obs.}$ (Å)	$d_{calc.}$ (Å)	I/I_o*	hkl	$d_{obs.}$ (Å)	$d_{calc.}$ (Å)	I/I_o*
2 1 1	6.697	6.699	104	0 6 10	2.7465	2.7488	8
2 2 0	6.099	6.094	1000	3 5 8		2.7442	32
0 4 0	5.929	5.930	420	1 8 5	2.7153	2.7138	22
1 2 7	4.678	4.685	23	0 8 6	2.6887	2.6885	43
2 1 7	4.267	4.260	39	2 7 7	2.6666	2.6688	19
1 5 4	4.068	4.072	24	5 3 2	2.6474	2.6480	36
0 6 2	3.869	3.872	5	3 7 4		2.6480	22
1 4 7		3.866	40	2 4 12	2.6122	2.6107	181
2 5 3	3.771	3.769	44	4 0 10	2.6034	2.6023	26
0 2 10	3.641	3.640	8	1 5 12		2.6007	34
4 0 2	3.486	3.492	10	1 9 2	2.5655	2.5681	10
1 6 5	3.409	3.409	52	2 6 10		2.5635	22
2 0 10	3.369	3.367	30	1 8 7		2.5633	24
4 2 2	3.345	3.349	14	4 2 10	2.5419	2.5419	21
1 3 10		3.346	31	1 3 14		2.5403	8
1 5 8	3.276	3.277	68	3 3 12	2.5061	2.5074	55
1 7 2	3.250	3.248	26	0 6 12	2.4810	2.4812	132
1 2 11		3.248	17	3 6 9	2.4668	2.4696	24
4 2 4	3.205	3.205	11	5 2 7		2.4656	15
2 5 7		3.198	26	4 7 1	2.4448	2.4467	15
0 0 12	3.182	3.187	39	4 6 6		2.4406	40
2 1 11	3.093	3.096	45	5 4 5	2.4298	2.4296	23
3 3 8		3.096	30	5 1 8		2.4295	30
0 2 12	3.079	3.078	36	0 10 2	2.3531	2.3541	9
3 2 9	3.058	3.056	91	1 10 1	2.3337	2.3354	23
4 4 0	3.048	3.047	39	6 2 0	2.3233	2.3218	55
2 4 10	2.9294	2.9281	12	3 5 12	2.3067	2.3095	41
1 5 10	2.9131	2.9141	33	1 7 12	2.2917	2.2912	42
2 5 9	2.8910	2.8912	55	4 8 0	2.2770	2.2761	56
1 6 9	2.8364	2.8362	50	2 10 0	2.2505	2.2500	84
5 1 2	2.7894	2.7907	16	4 4 12		2.2023	14
3 4 9		2.7905	32	4 5 11	2.2000	2.2009	15
5 2 1	2.7539	2.7558	25	6 4 0		2.1988	6

* The intensities are calculated from the Lazy Pulverix program (*5*).

TABLE II

MICROPROBE ANALYSIS (AVERAGE OF FIVE ANALYSIS POINTS)

	Nb	Se	Br
1	22.45	64.63	12.92
2	22.45	64.33	13.22
3	22.71	64.17	13.12
4	23.32	63.88	12.80
5	22.20	64.08	13.70

Experimental—Average values
Nb: 22.62(38)%, Se: 64.22(25)%, Br: 13.16(32)%
Theoretical $Nb_3Se_{10}Br_2$
Nb: 22.70%, Se: 64.29%, Br: 13.01%
Theoretical Nb_2Se_7Br ($|NbSe_4|+|NbSe_3Br|$)
Nb: 22.70%, Se: 67.53%, Br: 9.76%
Theoretical $Nb_2Se_6Br_2$ ($|NbSe_4|+|NbSe_2Br_2|$)
Nb: 22.68%, Se: 57.82%, Br: 19.50%

Such a formulation could not in the present case be unambiguously established from the structural determination due to the difficulty of assigning some atomic positions either to bromine or selenium (Br^- and Se^{2-} cannot be distinguished by X rays). In a first approach, on the basis of the recognition of Se–Se pairs and typical Nb–Br and Nb–Se bonds, the structural determination, as described below, leads to $|NbSe_4|_\infty$ and "$|NbSe_3Br|_\infty$" chains in a 1:1 ratio. Starting from this theoretical Nb_2Se_7Br composition, the real $Nb_3Se_{10}Br_2$ formulation must come from a particular Se → Br substitution on the "$|NbSe_3Br|_\infty$" chain.

The data were collected with a CAD4 Enraf–Nonius diffractometer using Mo$K\alpha$ radiation. Most of the experimental conditions are given in Table III. The data were treated in the usual fashion for Lorentz and polarization effects. A correction for absorption was also applied according to the approximate size (see Table III) of the crystal (flattened needle bound by {010}, {$\bar{1}$10}, and {001}).

TABLE III

1. Physical and crystallographic data
   - Formula: $Nb_3Se_{10}Br_2$; Molecular weight: 1228.1
   - Crystal symmetry: orthorhombic; Space group: *Ibca*
   - Cell parameters (293 K)
     - a = 14.205(3) Å
     - b = 23.722(4) Å
     - c = 38.243(8) Å
     - V = 12887 Å^3
     - Z = 32
   - Density d_{cal} = 5.06
   - Absorption factor μ(λ Mo$K\alpha$): 291 cm^{-1}
   - Crystal size 0.05 × 0.012 × 0.8 mm^3

2. Data collection
   - Temperature: 293 K; Radiation: Mo$K\alpha$
   - Monochromator: Oriented graphite (002); Scan mode: ω
   - Recording angle range: 2–35°; Scan angle: 1.00 + 0.40 tan θ
   - Values determining the scan speed
     - SIGPRE 0.5
     - SIGMA 0.01
     - VPRE 5° min^{-1}
     - T_{MAX} 100 s
   - Standard reflection 4 0 10, 0 6 12, $\bar{4}$ 0 10 Periodicity: 1 h

3. Refinement conditions
   - Reflections for the refinement of the cell dimensions 25
   - Recorded reflections in the eighth-space $\bar{h}$,0; 0,k; 0,l
   - Utilized reflections 2850 with $I \geq 4\sigma(I)$
   - Refined parameters 277
   - Reliability factors $R = \Sigma||F_o|-|F_c||/\Sigma|F_o|$
     $R_w = [\Sigma w(|F_o|-|F_c|)^2/\Sigma wF_o^2]^{1/2}$

4. Refinement results
   - R = 0.032 R_w = 0.034
   - Extinction coefficient E_c = 7.9 10^{-9}
   - Difference Fourier maximum peak intensity ±1.5(2) e^-/Å^3

The structure was solved by means of direct methods using a MULTAN 11/82 version (*7*) and subsequent Fourier syntheses. In the solution 2850 independent reflections ($I > 4\sigma I$), restricted to the $\sin\theta/\lambda$ range 0.15–0.65, were used. Refinement was carried out by the full-matrix least-squares method where the minimized quantity is $\Sigma w\|F_o|-|F_c\|^2$; a unit weight was applied for all reflections. After several cycles in which the anisotropic thermal parameters and a secondary extinction correction were refined, the R factors stabilize to $R = 0.032$ and $R_w = 0.034$. The difference Fourier map showed random peaks, the highest one reaching 1.5(2) $e^- \cdot$ Å^{-3}. Atomic coordinates and thermal parameters along with the interatomic distances are given in Tables IV and V. A list of the observed and calculated structure factors can be requested from the authors.

All calculations were performed with SDP Enraf–Nonius programs written by Frenz (*8*).

TABLE IV

POSITIONAL PARAMETERS AND THEIR ESTIMATED STANDARD DEVIATIONS

Atom	Position	x	y	z	B_{eq} (Å^2)
Nb1	8e	0	1/4	0.03310(5)	1.95(4)
Nb2	8e	0	1/4	0.11813(5)	2.05(4)
Nb3	8e	0	1/4	0.19934(5)	2.25(4)
Nb4	8e	0	1/4	0.28229(5)	2.56(4)
Nb5	8e	0	1/4	0.36765(5)	2.25(4)
Nb6	8e	0	1/4	0.44892(5)	2.12(4)
Nb7	8d	1/4	0.0307 (1)	0	4.19(5)
Nb8	16f	0.2361(1)	-0.00384(7)	0.08297(4)	3.36(3)
Nb9	16f	0.1757(1)	0.01867(7)	0.16525(6)	4.20(4)
Nb10	8c	0.2291(2)	0	1/4	3.88(5)
Se1	16f	0.1504(1)	-0.04906(7)	0.02817(4)	2.50(3)
Se2	16f	0.1057(1)	0.04128(8)	0.04376(4)	2.32(3)
Se3	16f	0.2351(1)	0.09154(7)	0.11721(4)	2.53(3)
Se4	16f	0.3421(1)	0.02491(8)	0.13754(4)	2.64(3)
Se5	16f	0.2485(1)	-0.06849(7)	0.19611(4)	2.54(3)
Se6	16f	0.0950(1)	-0.04629(8)	0.21320(4)	2.41(3)
Se7	16f	0.1375(1)	0.21929(8)	0.07199(4)	2.63(3)
Se8	16f	-0.0075(1)	0.34008(7)	0.07883(4)	2.53(3)
Se9	16f	0.1243(1)	0.30100(8)	0.15572(5)	2.87(4)
Se10	16f	0.1280(1)	0.20297(8)	0.16142(4)	2.89(4)
Se11	16f	0.1392(1)	0.28342(8)	0.24421(4)	3.11(4)
Se12	16f	0.0065(2)	0.34006(7)	0.23830(4)	3.11(4)
Se13	16f	0.1192(1)	0.19666(9)	0.32113(5)	3.42(4)
Se14	16f	-0.0373(2)	0.16301(8)	0.32600(5)	3.45(4)
Se15	16f	0.1431(1)	0.27411(9)	0.40793(5)	3.30(4)
Se16	16f	0.0944(1)	0.18046(8)	0.40778(5)	3.22(4)
Se17	16f	0.0314(1)	0.33708(7)	0.48923(4)	2.42(3)
Se18	16f	0.1220(1)	0.19814(8)	0.49462(4)	2.54(3)
Se A	16f	0.3760(1)	0.03620(9)	0.04845(5)	3.15(4)
Se B	16f	0.0994(1)	-0.04644(8)	0.11935(4)	2.72(3)
Se C	16f	0.2295(2)	0.09129(8)	0.21251(5)	3.56(4)
Br1	8d	1/4	0.1421 (1)	0	3.13(5)
Br2	16f	0.3160(2)	-0.10192(9)	0.08609(6)	4.00(4)
Br3	16f	0.0149(1)	0.07262(8)	0.16279(5)	3.12(4)
Br4	8c	0.4098(2)	0	1/4	4.29(7)

$$B_{eq} = 4/3 \sum_i \sum_j \beta_{ij} a_i a_j.$$

TABLE V

GENERAL TEMPERATURE FACTOR EXPRESSIONS—U's

Atom	U_{11}	U_{22}	U_{33}	U_{12}	U_{13}	U_{23}
Nb1	0.0222(9)	0.027 (1)	0.0246(9)	0.0004(9)	0	0
Nb2	0.0278(9)	0.0253(9)	0.0249(9)	0.001 (1)	0	0
Nb3	0.035 (1)	0.026 (1)	0.0245(9)	-0.000 (1)	0	0
Nb4	0.038 (1)	0.032 (1)	0.0266(9)	0.001 (1)	0	0
Nb5	0.0280(9)	0.029 (1)	0.0286(9)	0.002 (1)	0	0
Nb6	0.0230(9)	0.030 (1)	0.0279(9)	0.001 (1)	0	0
Nb7	0.038 (1)	0.033 (1)	0.087 (2)	0	0.029 (1)	0
Nb8	0.0471(9)	0.0302(7)	0.0506(8)	0.0079(8)	-0.0179(8)	-0.0066(8)
Nb9	0.0373(8)	0.0410(9)	0.081 (1)	0.0045(8)	0.0120(9)	0.0299(9)
Nb10	0.032 (1)	0.054 (1)	0.062 (1)	0	0	-0.031 (1)
Se1	0.0366(9)	0.0326(9)	0.0259(8)	-0.0053(8)	0.0018(7)	-0.0025(8)
Se2	0.0289(8)	0.0344(9)	0.0249(7)	0.0016(8)	0.0032(7)	0.0020(7)
Se3	0.045 (1)	0.0273(8)	0.0235(7)	-0.0022(8)	0.0035(8)	0.0005(7)
Se4	0.0341(8)	0.0414(9)	0.0248(7)	-0.0036(8)	-0.0010(8)	0.0038(8)
Se5	0.0430(9)	0.0314(8)	0.0223(7)	0.0030(8)	0.0013(8)	-0.0005(7)
Se6	0.0349(8)	0.0315(9)	0.0252(7)	-0.0049(8)	-0.0007(7)	0.0016(8)
Se7	0.0234(8)	0.049 (1)	0.0279(8)	0.0068(8)	-0.0021(7)	-0.0006(8)
Se8	0.0455(9)	0.0261(8)	0.0246(7)	0.0020(9)	-0.0000(8)	0.0016(7)
Se9	0.0416(9)	0.041 (1)	0.0270(8)	-0.0109(9)	-0.0029(8)	0.0004(8)
Se10	0.0429(9)	0.042 (1)	0.0250(8)	0.0148(8)	-0.0028(8)	-0.0025(8)
Se11	0.0413(9)	0.051 (1)	0.0261(9)	-0.0100(9)	0.0002(8)	-0.0026(8)
Se12	0.067 (1)	0.0252(8)	0.0262(7)	0.001 (1)	0.0032(9)	-0.0016(7)
Se13	0.049 (1)	0.051 (1)	0.0296(8)	0.0208(9)	-0.0012(8)	-0.0042(9)
Se14	0.068 (1)	0.0339(9)	0.0288(9)	-0.008 (1)	-0.0033(9)	0.0019(8)
Se15	0.0240(8)	0.069 (1)	0.0327(8)	-0.0103(9)	0.0005(8)	-0.003 (1)
Se16	0.050 (1)	0.047 (1)	0.0255(8)	0.0193(9)	-0.0029(9)	-0.0029(9)
Se17	0.0379(9)	0.0272(8)	0.0269(8)	-0.0037(7)	0.0017(7)	0.0004(7)
Se18	0.0276(8)	0.0406(9)	0.0283(9)	0.0087(8)	-0.0003(7)	-0.0010(8)
Se A	0.0352(9)	0.059 (1)	0.0259(8)	-0.0047(9)	0.0032(8)	0.0055(9)
Se B	0.0389(9)	0.041 (1)	0.0235(7)	-0.0073(8)	0.0051(8)	-0.0004(8)
Se C	0.075 (1)	0.036 (1)	0.0240(8)	-0.009 (1)	-0.0118(9)	0.0027(8)
Br1	0.032 (1)	0.034 (1)	0.053 (1)	0	0.008 (1)	0
Br2	0.044 (1)	0.034 (1)	0.074 (1)	0.0101(9)	-0.005 (1)	0.002 (1)
Br3	0.043 (1)	0.0352(9)	0.0400(9)	0.0071(8)	-0.0003(9)	-0.0009(8)
Br4	0.029 (1)	0.074 (2)	0.060 (2)	0	0	-0.002 (2)

The form of the anisotropic thermal parameter is:

$$\exp[-2\pi^2(h^2a^{*2}U_{11} + k^2b^{*2}U_{22} + l^2c^{*2}U_{33} + 2hka^*b^*U_{12} + 2hla^*c^*U_{13} + 2klb^*c^*U_{23})]$$

where a^*, b^*, c^* are reciprocal lattice constants.

Description and Discussion of the Structure

This structure can be described in terms of chains, running in a direction parallel to the c axis. Two types of chains are observed, being centered either on the 2 or on the 2_1 axes, respectively, as shown in the projection on the (a, b) plane (see Fig. 1). The first type consists of $|NbSe_4|_\infty$ chains built up from an infinite condensation of $[NbSe_8]$ rectangular antiprisms (Fig. 2). These chains are centered on the twofold axes. The second type is represented by pseudo-"$|NbSe_3Br|_\infty$" chains made up from the stacking, in a helicoidal way, of "$[NbSe_6Br]$" units by sharing a "$[Se_3]$" triangular base. This kind of chain is located around the 2_1 axes (Fig. 2).

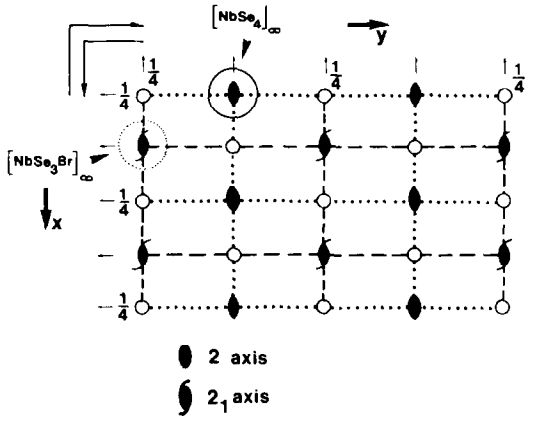

FIG. 1. Arrangement of $|NbSe_4|_\infty$ and "$|NbSe_3Br|_\infty$" chains on the 2 and 2_1 axes, respectively.

The $|NbSe_4|_\infty$ chains (see Fig. 3) look like those present in the $(MSe_4)_nI$ structural type (*4*). Niobium atoms are surrounded by eight selenium atoms in a rectangular antiprismatic arrangement. Two adjacent rectangular $[Se_4]$ planes make a dihedral angle of about 54°, slightly larger than in the $(MSe_4)_nI$ series. Let us represent each $[Se_4]$ plane by an arrow pointing from its center to the midpoint of the short Se–Se side (Fig. 4a). Figure 4b shows a schematic view of the stacking sequence of $[Se_4]$ planes along the *c* axis. Six adjacent arrows rotate ~54° clockwise and the next six counterclockwise.

Molecular orbital (MO) calculations on $[NbSe_8]^{4-}$ groups as a function of the dihedral angle θ show that the energy goes through a minimum when $\theta = 45°$ (*9*). This corresponds to the weakest overlap of occupied π and π^* MOs of adjacent $[Se_4]$ units. This minimizes the repulsive interactions. Also at $\theta = 45°$, we have a nice set of symmetry-adapted orbitals, originating from the Se atoms, that interact with the metal orbitals except dz^2. The dz^2 orbital governs the electronic properties as a function of both its state of filling and the metal–metal distances along the chain.

The θ value observed here (~54°) is rather different from the ideal value (45°). A structural consequence is that since 360° is not an integral multiple of 54°, the rotation of the $[Se_4]$ rectangles with respect to each other has to be counterclockwise and clockwise. Such a situation was earlier mentioned for $(MSe_4)_nI$. Particularly, this was the case for $(NbSe_4)_3I$ (→ rotation sequence 123432) (*10*), and also for $(NbSe_4)_{10/3}I$ (→ 1234565432) (*11*).

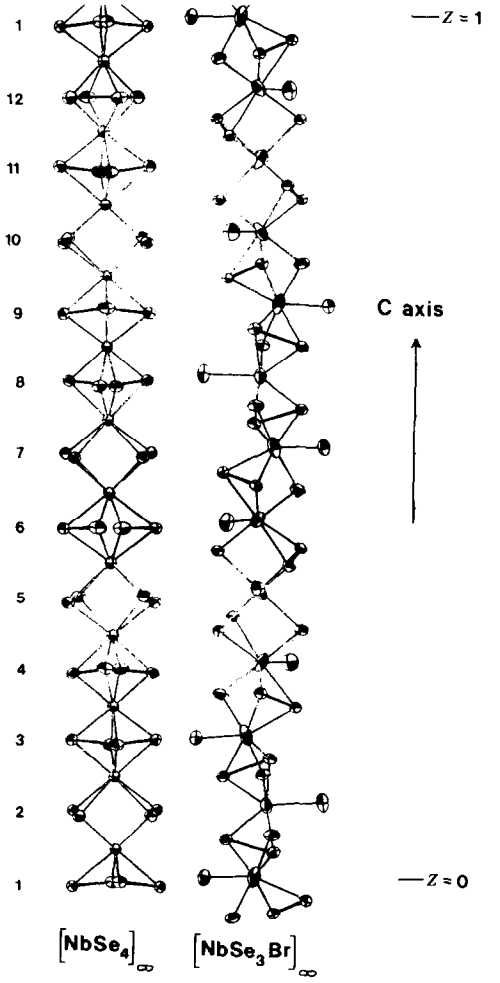

FIG. 2. A view of both types of chains seen orthogonal to (110).

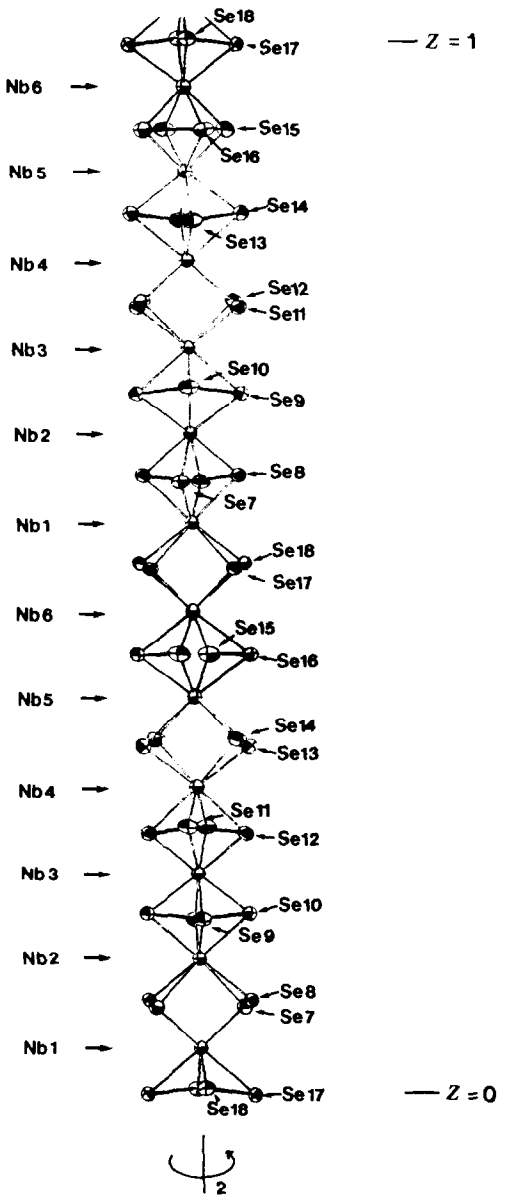

FIG. 3. Drawing of an individual $|NbSe_4|_\infty$ chain.

Band structure calculations will be done to understand the relative arrangement of the $[Se_4]$ rectangles and perhaps to provide an explanation for such a θ value.

Within the $|NbSe_4|_\infty$ chain, Nb–Nb bond lengths are arranged according to the sequence reported in Table VI. Comparable values are found in $(NbSe_4)_3I$ or $(NbSe_4)_{10/3}I$. The Nb–Se bond lengths range from about 2.56 to 2.76 Å (see Table VII), which is also in good agreement with the average values observed in similar compounds.

The "$|NbSe_3Br|_\infty$" type of chain greatly differs from the former one (Fig. 5). A first distinction comes from the coordination around niobium atoms. Selenium atoms are distributed at the corners of triangular antiprisms (irregular triangle with a short Se–Se bond of about 2.33 Å, typical of a Se_2^{2-} pair). Then, each niobium atom is capped by one bromine atom in a strong Nb–Br bond (see Table VIII and Fig. 6). This is reminiscent of what is occurring for niobium in $Nb_6Se_{20}Br_6$ (*12*) and for molybdenum in $Mo_3S_7Cl_4$ (*13*). In the latter case

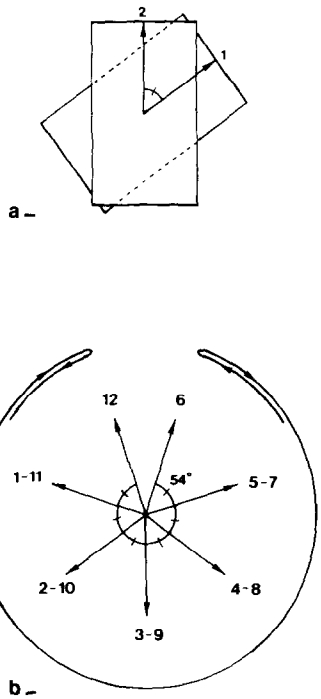

FIG. 4. (a) Relative orientation of adjacent $[Se_4]$ units. (b) Schematic diagram illustrating the numbered sequence of $[Se_4]$ units along the $|MSe_4|_\infty$ chain.

TABLE VI

Nb–Nb Bond Lengths along the Chains (Å)

A. $Nb_3Se_{10}Br_2 \rightarrow E_a = 0.34$ ev

(i) along the $|NbSe_4|_\infty$ chain ($\bar{l} = 3.187$ Å, $\sigma l = 0.063$ Å)

$$\cdots \; Nb1 \overset{3.252}{\text{——}} Nb2 \overset{3.106}{\text{——}} Nb3 \overset{3.172}{\text{——}} Nb4 \overset{3.264}{\text{——}} Nb5 \overset{3.108}{\text{——}} Nb6 \overset{3.219}{\text{——}} Nb1'$$

z values	0.03	0.12	0.20	0.28	0.37	0.45	0.53

(ii) along the "$|NbSe_3Br|_\infty$" chain ($\bar{l} = 3.313$ Å, $\sigma l = 0.028$ Å)

$$Nb8' \cdots \; Nb7 \overset{3.283}{\text{——}} Nb8 \overset{3.305}{\text{——}} Nb9 \overset{3.358}{\text{——}} Nb10 \overset{3.305}{\text{——}} Nb9'$$

z values	$z = 0$	0.25

B. $(NbSe_4)_3I \rightarrow E_a = 0.38$ eV

$$\overset{3.061}{\cdots} \; Nb \overset{3.252}{\text{——}} Nb \overset{3.252}{\text{——}} Nb \overset{3.061}{\text{——}} Nb \overset{3.252}{\text{——}}$$

($\bar{l} = 3.188$ Å, $\sigma l = 0.090$ Å)

C. $(NbSe_4)_{10/3}I \rightarrow E_a = 0.34$ eV

$$\text{——} Nb \overset{3.171}{\text{——}} Nb \overset{3.171}{\text{——}} Nb \overset{3.232}{\text{——}} Nb \overset{3.150}{\text{——}} Nb \overset{3.232}{\text{——}}$$

($\bar{l} = 3.191$ Å, $\sigma l = 0.034$ Å)

Note. $\bar{l} = \Sigma x/n$, $\sigma l = [(\Sigma x^2 - (\Sigma x)^2/n)/n]^{1/2}$.

TABLE VII

Interatomic Distances (Å) within the $|NbSe_4|_\infty$ Chains

Nb1–2Se17	2.698	Nb2–2Se7	2.731
–2Se18	2.585	–2Se8	2.615
–2Se7	2.562	–2Se9	2.578
–2Se8	2.763	–2Se10	2.701
Se17–Se18 = 2.343	Se7–Se8 = 2.338	Se9–Se10 = 2.336	
Nb3–2Se9	2.714	Nb4–2Se11	2.581
–2Se10	2.580	–2Se12	2.721
–2Se11	2.736	–2Se13	2.583
–2Se12	2.606	–2Se14	2.756
Se9–Se10 = 2.336	Se11–Se12 = 2.327	Se13–Se14 = 2.376	
Nb5–2Se13	2.763	Nb6–2Se15	2.630
–2Se14	2.615	–2Se16	2.645
–2Se15	2.614	–2Se17	2.616
–2Se16	2.622	–2Se18	2.752
Se13–Se14 = 2.376	Se15–Se16 = 2.327	Se17–Se18 = 2.343	
Nb1–Nb2	3.252	Nb4–Nb5	3.264
Nb2–Nb3	3.106	Nb5–Nb6	3.108
Nb3–Nb4	3.172	Nb6–Nb1′	3.219

Note. Standard deviations are all less than or equal to 10^{-3}.

there are, however, two chlorine atoms playing different roles; one is capping molybdenum, and the other is participating in a triangular S_2Cl group. These various types of coordination have been recognized and classified by Evain (*14*), who described the various ways to introduce chalcogen pairs around a metal.

The "$|NbSe_3Br|_\infty$" chain is made up by the juxtaposition of 12 $[NbSe_6Br]$ units along the *c* axis by sharing their triangular "Se_3" base. This framework looks like a spiral staircase when seen along the *c* axis (see Fig. 5). Bromine atoms which play the step role display the rotating sequence of adjacent units (from I to XII as shown in Fig. 7). Dihedral angles between successive bromine atoms are found to be equal to Br1–Nb–Br2 ~ 155°, Br2–Nb–Br3 ~ 145°, and Br3–Nb–Br4 ~ 150° (projection on the (*a*, *b*) plane). The corresponding Nb–Br distances (Table VIII) are similar to what is

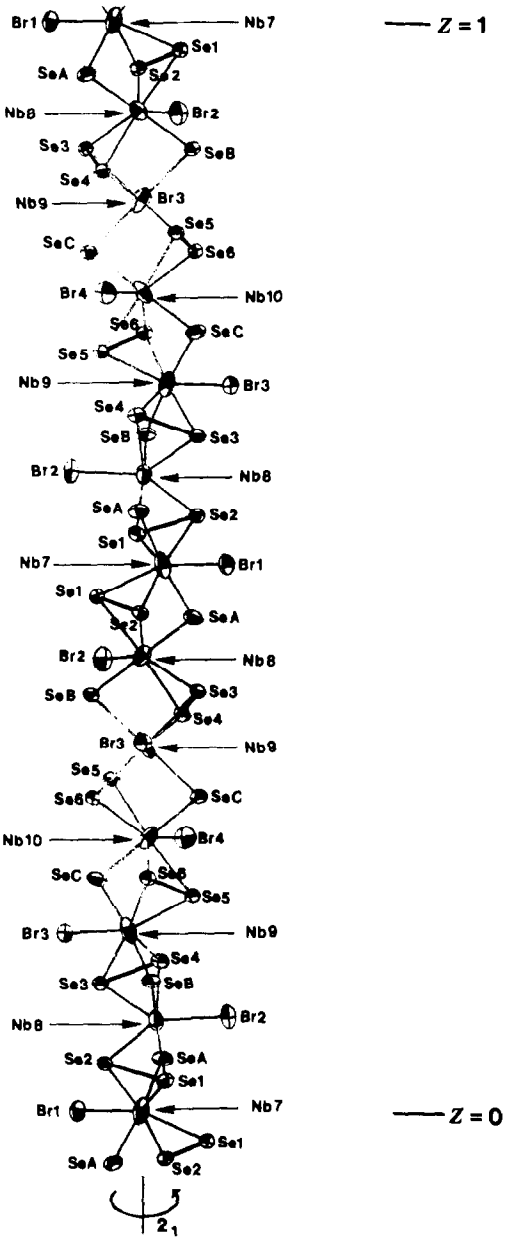

FIG. 5. Drawing of an individual "$|NbSe_3Br|_\infty$" chain.

usually observed, e.g., 2.692, 2.680, 2.685, and 2.674 Å in $Nb_6Se_{20}Br_6$ (*12*).

The only structural ambiguity arose as far as the positions noticed Se*A*, Se*B*, and Se*C* are concerned. As already mentioned above, the nature of the chemical species (bromine or selenium) which had to be located on Se*A*, Se*B*, or Se*C* positions could not be obtained from the structural study. According to the $Nb_3Se_{10}Br_2$ formulation, one-third of the Se*A*/Se*B*/Se*C* positions have to be occupied by bromine. This leads to [Se_3] triangles and [Se_2Br] triangles in a 2 : 1 ratio along that chain. Both kinds of these triangles have already been recognized (i) in $NbSe_3$ (*15*) (type III chain) for the [Se_3] triangle and (ii) in $Nb_6Se_{20}Br_6$ for the [Se_2Br] triangle.

The recent synthesis of $Nb_3Se_{10}Cl_2$ (*16*) indirectly confirms the existence of a $Nb_3Se_{10}X_2$ series. The structural determina-

TABLE VIII

INTERATOMIC DISTANCES (Å) WITHIN THE "$|NbSe_3Br|_\infty$" CHAIN

	$\|NbSe_6Br\|$ polyhedra		
Nb7–2Se1	2.596	Nb8 –Se1	2.650
–2Se2	2.658	–Se2	2.613
–2SeA	2.579	–Se3	2.614
–Br1	2.643	–Se4	2.662
		–SeA	2.568
		–SeB	2.594
		–Br2	2.592
Nb9–Se3	2.660	Nb10–2Se5	2.639
–Se4	2.595	–2Se6	2.610
–Se5	2.596	–2SeC	2.597
–Se6	2.655	–Br4	2.567
–SeB	2.577		
–SeC	2.611		
–Br3	2.620		
	"Se_3" triangular base		
Se1 –Se2	2.313	Se3 –Se4	2.327
Se1 –SeA	3.867	Se3 –SeB	3.799
Se2 –SeA	3.846	Se4 –SeB	3.903
Se5 –Se6	2.336		
Se5 –SeC	3.851		
Se6 –SeC	3.781		
Nb7–Nb8	3.283		
Nb8–Nb9	3.305		
Nb9–Nb10	3.358		

Note. Standard deviations are all less than or equal to 10^{-3}.

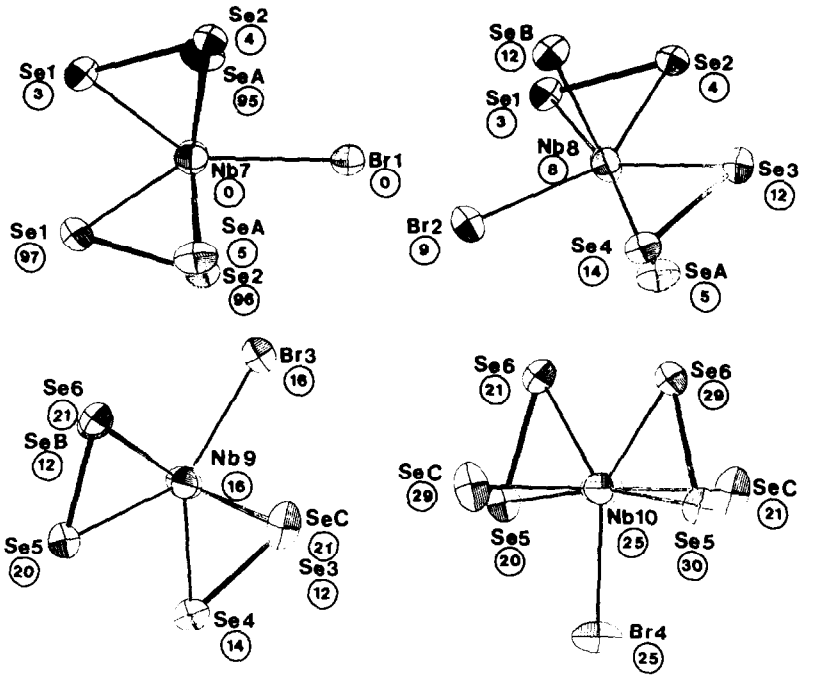

FIG. 6. Niobium atoms with trigonal antiprismatic monocapped coordinations in the "$|NbSe_3Br|_\infty$" chain.

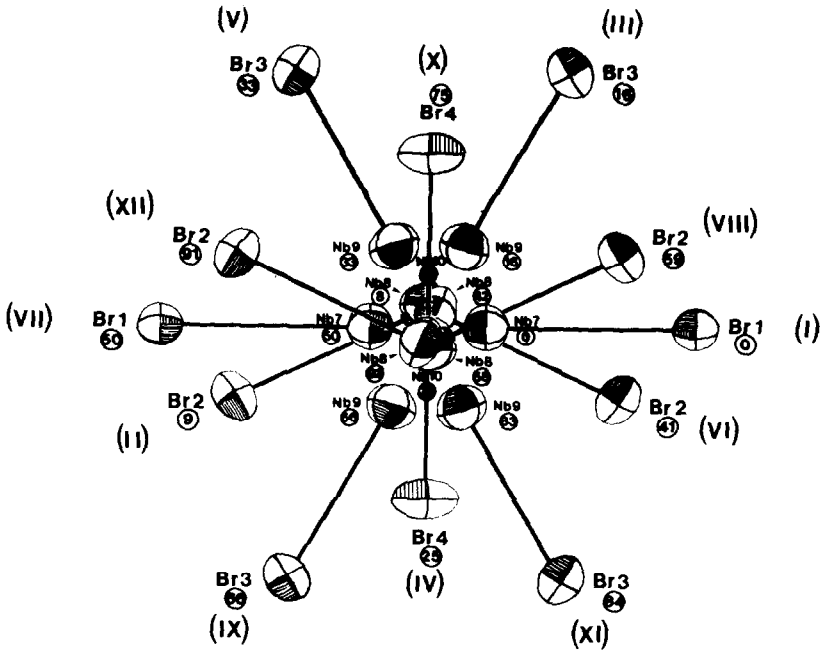

FIG. 7. Projection along [001] of Nb/Br atoms belonging to the "$|NbSe_3Br|_\infty$" chain.

tion now in progress will allow the determination in that case of the relative position of the $[Se_3]$ and $[Se_2X]$ triangles (ordered or disordered).

The other selenium positions are unambiguously assigned because they are engaged in $(Se_2)^{2-}$ pairs with the usual bond length of ~2.33 Å.

In the "$|NbSe_3Br|_\infty$" chain, niobium atoms are not exactly aligned along the c axis as they are, for instance, within the $|NbSe_4|_\infty$ chain. Three different Nb–Nb distances are observed according to the sequence reported in Table VI.

Interactions between the two types of chains could only be established through their nearest Br · · · Se or Se · · · Se atoms (see Table IX).

These bond values are, on the whole, greater than 3.3 Å, which indicates a rather weak interaction of the van der Waals type. But a shorter bond is observed between Se8 and Br2 (3.061 Å). Such a value, much lower than the sum (3.66 Å) of the van der Waals radii (Se^{2-} = 1.84 Å, Br^- = 1.82 Å) (*17*), addresses the question of the existence of a weak and covalent bonding between these atoms. Interanionic contacts of the same order of magnitude have already been observed in compounds such as V_2PS_{10} (*18*) and $V(S_2C_2Ph_2)$ (*19*) for instance. One finds S · · · S distances of 2.972 and 2.995 Å for the former phase and 2.927, 3.089, and 3.178 Å for the latter one.

TABLE IX

SHORTEST Se–Se AND Se–Br (<3.5) INTERCHAIN BOND LENGTHS (Å)

A. Between $\|NbSe_4\|_\infty$ and "$\|NbSe_3Br\|_\infty$" chains	
$\|NbSe_4\|_\infty$ $\|NbSe_3Br\|_\infty$	
Se8–Br2	3.061
Se10–Br3	3.485
Se16–SeB	3.345
Se17–Br1	3.173
B. Between two adjacent $\|NbSe_4\|_\infty$ chains	
Se15–Se7	3.215

Is that the beginning of the formation of polyanions? Molecular orbital calculations, made on these phases (*20*), showed that the overlap population for the corresponding interanionic contacts were all negative. Then, the occurrence of these short distances are not to be related to S · · · S bonds, but must be seen as the result of the constraints imposed to the sulfur ligands forced to be close to each other because of the high coordination (8) and the small size of "V^{4+}." It is actually observed that with a larger metal atom ("Nb^{4+}" or "Ta^{5+}" for instance) and in similar or related phases the phenomenon does not occur.

However, in $Nb_3Se_{10}Br_2$, a Br · · · Se distance as small as 3.061 Å cannot originate in any geometrical constraint as in the case of the above vanadium derivatives. Thus, the occurrence of a bonding interaction between these atoms cannot be rejected. A molecular orbital calculation already started should provide an answer to this question. It is necessary to emphasize that $Nb_3Se_{10}Br_2$ is not the first phase of the Nb–Se–Br system to present such small interanionic distances. For example, in $Nb_6Se_{20}Br_6$, Se · · · Br distances of 3.029, 3.179, 3.190, and 3.205 Å have also been calculated without any explanation of these features.

Physical Properties

Susceptibility

Magnetic susceptibility measurements have been performed on a collection of single crystals (21.7 mg) with a Faraday balance in the temperature range 300–100 K. After correction for the ion-core diamagnetism ($\chi_{dia} = -80.10^{-6}$ uem · mole^{-1}), the susceptibility is found to be diamagnetic (see Fig. 8); theoretical values reported by Bernier and Poix (*21*) have been used for the corrections (Table X).

A simple valence (ionic) assignment model can be proposed on the basis of

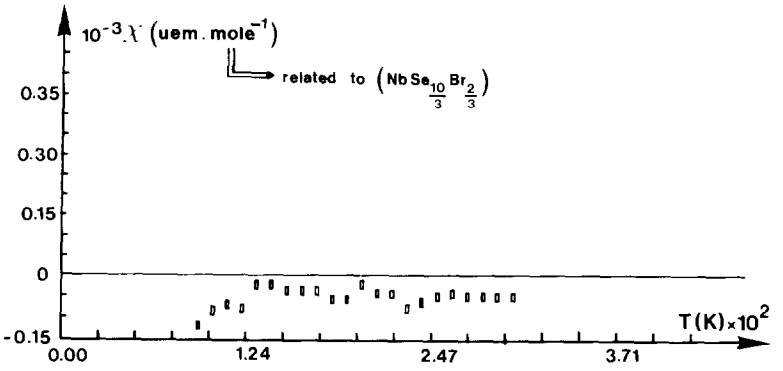

FIG. 8. Molar susceptibility versus temperature.

structural considerations: For the $|NbSe_4|_\infty$ chain

$$12[Nb, 2(Se_2^{2-})] \rightarrow (60\text{–}48 = 12\ d\text{-electrons}).$$

For the "$|NbSe_3Br|_\infty$" chain

$$[12Nb, 12(Se_2^{2-}) - 8Se^{2-} - 16Br^-] \rightarrow (60\text{–}56 = 4\ d\text{-electrons}).$$

This even number of d-electrons is usually taken to account in a first approach to explain the diamagnetism in these chain-like materials.

Resistivity

Resistivity measurements using the standard four-probe technique were performed on a needle-shaped crystal; the contacts were made with silver paint. Figure 9 shows the low-electric-field resistivity as a function of the inverse of temperature. $Nb_3Se_{10}Br_2$ is a diamagnetic semiconductor (E_a = 0.34 eV). This behavior is similar to what is observed for the parent chain-like compounds such as the $(MSe_4)_nI$ phases (*1*, *2*) (see Table VI).

TABLE X

CORRECTION FOR THE ION-CORE DIAMAGNETISM (THEORETICAL VALUES) ACCORDING TO BERNIER AND POIX (*21*)
$(-\chi \times 10^6)$

Nb^{4+}	21.6 emu · mol^{-1}
Nb^{5+}	12.9 emu · mol^{-1}
Se_2^{2-}	14.1 emu · mol^{-1}
Se^{2-}	47. emu · mol^{-1}
Br^-	36.7 emu · mol^{-1}

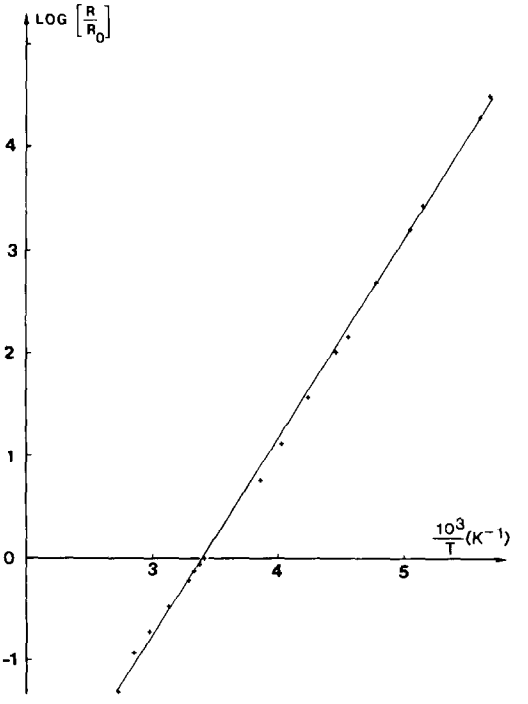

FIG. 9. Normalized resistance versus $10^3/T$.

Discussion and Conclusion

$Nb_3Se_{10}Br_2$ brings two new features in the solid state chemistry of pseudo-1-D compounds: (i) a new type of chain referred to as "$NbSe_3Br$" (in fact $Nb_3Se_8Br_4$) and (ii) a composite structure associating two kinds of chains, $|NbSe_4|_\infty$ and "$|NbSe_3Br|_\infty$."

The $|NbSe_4|_\infty$ chain is now well known since the structural determinations of $(MSe_4)_nI$ (M = Nb, Ta) have been reported. Such a chain has never been observed alone. Even under pressure, the synthesis of a $NbSe_4$ chain compound, homologous to VS_4, has been unsuccessful. The presence of a large anion is needed to stabilize the structure. Moreover, this anion (iodine) modulates the electronic density by pulling one electron out of the (MSe_4) chain and consequently modifying the dz^2 band filling and the associated $2k_F$ charge-density-wave-type distortions (*9*).

The "$NbSe_3Br$" type of chain retains some structural elements of both $|NbSe_3|_\infty$ and $|Nb_6Se_{20}Br_6|_\infty$ chains.

An important problem is the role of the "$|NbSe_3Br|_\infty$" chains between the $|NbSe_4|_\infty$ chains. It has obviously a geometric role which is to separate the $[MX_4]$ chains. Has it, also, a role involving an electronic exchange from chain to chain? No conclusion can be drawn at this time.

The transport properties are likely governed by the metal–metal intrachain overlap within the $|NbSe_4|_\infty$ chain. The Nb–Nb bond length along this chain has values between 3.11 and 3.26 Å (Table VI); similar band alternations have been noticed for $(NbSe_4)_3I$ and $(NbSe_4)_{10/3}I$ (see Table VI). It is thus not surprising to find very similar activation energies (0.38, 0.34, and 0.34 eV for $(NbSe_4)_3I$, $(NbSe_4)_{10/3}I$, and $Nb_3Se_{10}Br_2$, respectively. Band structure calculations will be done to determine the effect of interchain coupling along with the band filling of dz^2 orbitals for each compound.

Acknowledgments

We gratefully thank A. Ben Salem and P. Colombet for their technical assistance in resistivity and susceptibility measurements, respectively, and Professor R. Brec for helpful discussions.

References

1. P. Monceau, "Electronic Properties of Inorganic Quasi 1D Compounds," Parts I and II, Reidel, Dordrecht (1986).
2. J. Rouxel, "Crystal Chemistry and Properties of Quasi 1D Structures," Reidel, Dordrecht (1986).
3. A. Kutoglu and R. Allman, *Neues Jahrb. Miner. Monat. H* **8,** 339 (1972).
4. P. Gressier, A. Meerschaut, L. Guémas, J. Rouxel, and P. Monceau, *J. Solid State Chem.* **51,** 141 (1984).
5. K. Yvon, W. Jeitschko, and E. Parthe, *J. Appl. Crystallogr.* **10,** 73 (1977).
6. J. Rijnsdorp, Ph.D. thesis, University of Groningen, Groningen (1978).
7. P. Main, MULTAN program 11/82 version (July 1982).
8. B. Frenz, "Enraf–Nonius, Structure Determination Package," Delft Univ. Press, Delft, 1983.
9. P. Gressier, M.-H. Whangbo, A. Meerschaut, and J. Rouxel, *Inorg. Chem.* **23,** 1221 (1984).
10. A. Meerschaut, P. Palvadeau, and J. Rouxel, *J. Solid State Chem.* **20,** 21 (1977).
11. A. Meerschaut, P. Gressier, L. Guémas, and J. Rouxel, *J. Solid State Chem.* **51,** 307 (1984).
12. A. Meerschaut, P. Grenouilleau, and J. Rouxel, *J. Solid State Chem.* **61,** 90 (1986).
13. J. Fenner, A. Rabenau, and G. Trageser. *Adv. Inorg. Chem. Radiochem.* **23,** 329 (1980).
14. M. Evain, to be published.
15. A. Meerschaut and J. Rouxel, *J. Less-Common Metals* **39,** 197 (1975).
16. L. Guémas, A. Zadane, A. Meerschaut, and P. Palvadeau, unpublished results.
17. R. D. Shannon, *Acta Crystallogr. A* **32,** 751 (1976).
18. R. Brec, G. Ouvrard, M. Evain, P. Grenouilleau, and J. Rouxel, *J. Solid State Chem.* **47,** 174 (1983).
19. R. Eisenberg and M. B. Gray, *Inorg. Chem.* **6,** 1844 (1967).
20. M. Evain, R. Brec, and M.-H. Whangbo, *J. Solid State Chem.* (1986).
21. J. C. Bernier and P. Poix, *L'Actualité Chim.* **7,** (1978).